



Patterning of Thick Parylene Films by Oxygen Plasma for Application as Exploding Foil Initiator Flyer Material

by Eugene Zakar and Michael D. Grapes

ARL-TR-4956

September 2009

NOTICES

Disclaimers

The findings in this report are not to be construed as an official Department of the Army position unless so designated by other authorized documents.

Citation of manufacturer's or trade names does not constitute an official endorsement or approval of the use thereof.

Destroy this report when it is no longer needed. Do not return it to the originator.

Army Research Laboratory

Adelphi, MD 20783-1197

ARL-TR-4956

September 2009

Patterning of Thick Parylene Films by Oxygen Plasma for Application as Exploding Foil Initiator Flyer Material

**Eugene Zakar and Michael D. Grapes
Sensors and Electron Devices Directorate, ARL**

REPORT DOCUMENTATION PAGE			Form Approved OMB No. 0704-0188		
<p>Public reporting burden for this collection of information is estimated to average 1 hour per response, including the time for reviewing instructions, searching existing data sources, gathering and maintaining the data needed, and completing and reviewing the collection information. Send comments regarding this burden estimate or any other aspect of this collection of information, including suggestions for reducing the burden, to Department of Defense, Washington Headquarters Services, Directorate for Information Operations and Reports (0704-0188), 1215 Jefferson Davis Highway, Suite 1204, Arlington, VA 22202-4302. Respondents should be aware that notwithstanding any other provision of law, no person shall be subject to any penalty for failing to comply with a collection of information if it does not display a currently valid OMB control number.</p> <p>PLEASE DO NOT RETURN YOUR FORM TO THE ABOVE ADDRESS.</p>					
1. REPORT DATE (DD-MM-YYYY) September 2009		2. REPORT TYPE Progress		3. DATES COVERED (From - To) June to August 2008	
4. TITLE AND SUBTITLE Patterning of Thick Parylene Films by Oxygen Plasma for Application as Exploding Foil Initiator Flyer Material			5a. CONTRACT NUMBER		
			5b. GRANT NUMBER		
			5c. PROGRAM ELEMENT NUMBER		
6. AUTHOR(S) Eugene Zakar and Michael D. Grapes			5d. PROJECT NUMBER		
			5e. TASK NUMBER		
			5f. WORK UNIT NUMBER		
7. PERFORMING ORGANIZATION NAME(S) AND ADDRESS(ES) U.S. Army Research Laboratory ATTN: RDRL-SER-L 2800 Powder Mill Road Adelphi, MD 20783-1197			8. PERFORMING ORGANIZATION REPORT NUMBER ARL-TR-4956		
9. SPONSORING/MONITORING AGENCY NAME(S) AND ADDRESS(ES) U.S. Army TACOM-ARDEC Fuze Division 2800 Powder Mill Road Adelphi, MD 20783-1197			10. SPONSOR/MONITOR'S ACRONYM(S)		
			11. SPONSOR/MONITOR'S REPORT NUMBER(S)		
12. DISTRIBUTION/AVAILABILITY STATEMENT Approved for public release; distribution unlimited.					
13. SUPPLEMENTARY NOTES					
14. ABSTRACT Parylene is an attractive flyer material for the exploding foil initiator due to its superior conformal step coverage and inert properties. A process for patterning thick films of Parylene using a thin metal masking layer and oxygen plasma has been developed. Gold and titanium have been compared as masking materials on the basis of masking quality and compatibility with existing processes. Etch rate, directionality, and minimum feature size have been approximated for isotropic and anisotropic oxygen plasma etch recipes. Remaining obstacles to process integration are discussed.					
15. SUBJECT TERMS Fuze, EFI, parylene, oxygen plasma					
16. SECURITY CLASSIFICATION OF:			17. LIMITATION OF ABSTRACT UU	18. NUMBER OF PAGES 24	19a. NAME OF RESPONSIBLE PERSON Eugene Zakar
a. REPORT Unclassified	b. ABSTRACT Unclassified	c. THIS PAGE Unclassified			19b. TELEPHONE NUMBER (Include area code) (301) 394-1628

Contents

List of Figures	iv
List of Tables	v
1. Introduction/Background	1
2. Experiment/Calculations	4
2.1 Parylene Etch Rate Calculation	4
2.2 Metal Masking Feasibility	5
2.3 Etch Characterization	6
3. Results and Discussion	7
3.1 Parylene Etch Rate Calculation	7
3.2 Metal Masking Material Feasibility	7
3.2.1 Ti Masking	7
3.2.2 Au Masking	8
3.3 Etch Characterization	11
3.4 Outstanding Issues.....	12
4. Summary and Conclusions	13
5. References	14
List of Symbols, Abbreviations, and Acronyms	15
Distribution List	16

List of Figures

Figure 1. Photograph of a typical EFI (top view).	1
Figure 2. Schematic illustration side view of the flyer material operation in an EFI: a) a thin film copper (Cu) bridge and Parylene flyer material in line with the secondary, awaiting the firing signal; b) upon the fire command, the Cu bridge vaporizes and the Parylene flyer is sheared off and launched toward secondary explosive; and c) the flyer impacts the secondary explosive and the subsequent shockwave initiates detonation.	1
Figure 3. Chemical structures for different types of Parylene.	3
Figure 4. Process flow for patterning Parylene with a metal mask.	4
Figure 5. Optical microscope images of metal mask patterns on silicon substrate: (a) crosses, (b) squares and dots, and (c) lines.	6
Figure 6. Plots of average Parylene step height versus time for (a) isotropic and (b) anisotropic etch recipe. Note the generally linear trend.	7
Figure 7. Scanning electron micrograph showing the edge of a Ti mask and underlying Parylene film after anisotropic oxygen plasma etch. Note good pattern transfer as well as good Parylene step coverage over the Cu bridge structure. Stringy clumps in the lower right are as yet unidentified etch residues, possibly related to etch chamber contamination.....	8
Figure 8. Optical microscope images showing complications after the process of removing the Ti mask. In (a), the dot patterned Parylene film shows striations and discoloration along the edge of a metal Cu bridge that are indicative of peeling, while in (b), the Parylene dot film has been completely removed.	8
Figure 9. Dimensions of the mask cross patterns prior to etching. The upper cross (a) is slightly larger than the lower cross (b).	9
Figure 10. Micrographs illustrating varying degrees of etch undercutting below the Au mask: (a) optical microscope image showing the Au mask patterns prior to Parylene etching, (b) SEM corner of large cross pattern transfer after anisotropic etch, (c) the same corner after isotropic etch (note greater undercutting), (d) SEM of two smaller crosses after anisotropic etch, and e) the same crosses after isotropic etch (the smaller cross has been completely undercut).	10
Figure 11. Cracking of Parylene film from the isotropic etch recipe. Multiple cracking is evident in the partially etched Parylene film as well as through the Au masking layer.	11
Figure 12. Scanning electron micrograph overview of anisotropic etched features 200, 150, 100, 60, 40, 20, 10, and 5 μm (from top to bottom).	12
Figure 13. Scanning electron micrographs depicting the approximate minimum feature size of line patterns after anisotropic etch: (a) 1000 times magnification of 10- μm -wide lines and (b) 600 times magnification of 5- μm -wide lines.	12

List of Tables

Table 1. Oxygen plasma etch recipes tested.	5
--	---

INTENTIONALLY LEFT BLANK.

1. Introduction/Background

Microelectromechanical system (MEMS) exploding foil initiator (EFI) type fuzes are being explored to improve the performance and satisfy the requirements of MIL-STD-1316E, which mandates that any electrical fuze initiating an “uninterruptable explosive train” leading to ignition of the main charge in a warhead requires a voltage in excess of 500 V to fire. In the EFI an electrical current travels through a wide conductor path until it crosses a narrow neck, a.k.a. bridge, shown in figure 1, where it vaporizes and starts a chain of events with the flyer material. A reliable flyer material needs to be robust, able to withstand an impulsive launch, and remain intact at speeds approaching supersonic velocity. The operational sequence of events leading to detonation of an insensitive secondary explosive is illustrated in figure 2. EFIs eliminate the use of a sensitive primary explosive by requiring a voltage of 3000–4000 V for detonation, easily satisfying the 500 V requirement.

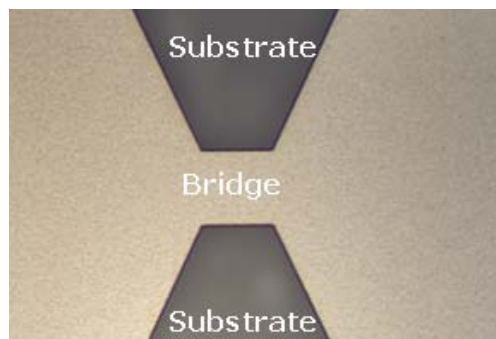


Figure 1. Photograph of a typical EFI (top view).

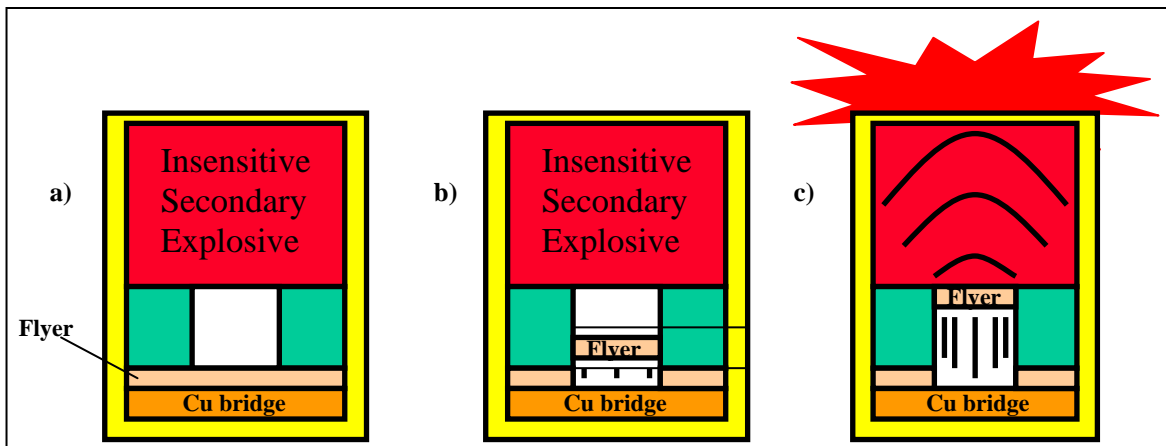


Figure 2. Schematic illustration side view of flyer material operation in an EFI: a) a thin film copper (Cu) bridge and Parylene flyer material in line with the secondary, awaiting the firing signal; b) upon the fire command, the Cu bridge vaporizes and the Parylene flyer is sheared off and launched toward secondary explosive; and c) the flyer impacts the secondary explosive and the subsequent shockwave initiates detonation.

Parylene can be used as a flyer material and has several distinct advantages over other polymer materials, Kapton, and polyimide materials, due to its superior step coverage over circuit topography and inert quality owing to its low outgassing properties. These characteristics improve the performance, predictability, and stability of the EFI. The thickness requirement for a flyer material can vary depending on the energy requirements of the initiator, as it must be robust during launch, but generally speaking, it is near 1 mil ($\sim 25\text{ }\mu\text{m}$). We use the term “thick” film Parylene for this application, because in comparison to other applications in integrated circuits “thin” films are generally near $1\text{ }\mu\text{m}$.

Currently, Parylene type “C” can only be chemical vapor deposited over the entire circuit surface, and selective removal is achieved only by taping the substrate surface prior to deposition and then peeling it off after the deposition. This method is inherently imprecise, and produces very uneven cut and dirty surfaces compared to clean room processing practices. An easily integrated process for patterning Parylene is needed to achieve high reliability and reproducibility both in production and use.

The Parylenes (poly-*p*-xylylene and its derivatives) are polymeric films. They are chemical vapor deposited in a process originally developed by W. F. Gorham (1), in which Parylene dimer (di(poly-*p*-xylylene)) is vaporized ($\sim 165\text{ }^{\circ}\text{C}$), pyrolyzed to the monomer poly-*p*-xylylene ($\sim 670\text{ }^{\circ}\text{C}$), and then deposited at room temperature. The mechanism of deposition is given by Gazicki-Lipman as beginning with condensation of Parylene monomer on and diffusion to the surface, followed by chain initiation and propagation, in which the monomer molecules form long polymer chains (2). The activation energy for adding a monomer unit to an existing chain (propagation) is much lower than for the binding of the first two monomer units (initiation), so this deposition method tends to produce very high molecular weight polymers. Since polymerization is preceded by condensation, the Parylenes are highly transparent, conformal, pinhole-free coatings over large surface areas.

The commercial name for unsubstituted poly-*p*-xylylene is Parylene N, known for its excellent dielectric properties. Monochloro-substituted Parylene C, used in this work, contains a single additional chlorine atom on the benzene ring. Parylene C is thermally stable and chemically inert, and is often used to passivate sensitive devices against hostile environments. Dichloro-substituted Parylene D is also available. The chemical structures of the Parylenes are shown in figure 3.

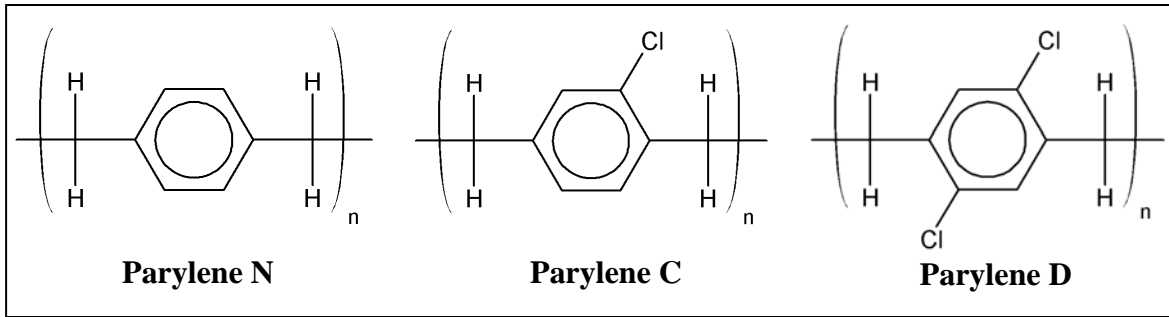


Figure 3. Chemical structures for different types of Parylene.

Unfortunately, the beneficial properties of Parylene C also complicate its patterning. Because it is chemically inert, a selective wet etch for Parylene does not exist. It cannot be patterned using conventional lift-off techniques, because it deposits very conformally over features. Some research has been done in the area of laser ablation of Parylene films for microelectrode tips (3), but this method is not suited for large (i.e., wafer-scale) patterning and would require investment in or construction of specialized equipment. Oxygen plasma is an attractive method for Parylene patterning. Oxygen plasma processes are frequently used for photoresist ashing and descum, so commercial tools to perform this process are already available.

Plasma etching of silicon (using SF_6 plasma) or silicon dioxide (using CF_4 or CHF_3 plasmas) can be accomplished using photoresist as a masking layer since these plasmas selectively etch only the target material. However, the selectivity between photoresist and Parylene in oxygen plasma is near unity, so for a thick film of Parylene an alternative masking layer is preferable to prevent the mask from eroding away before the completion of the etch. Metals are known to have a negligible etch rate in oxygen plasma and can be very good as a masking material for Parylene etching. Fine-line patterning of the metal masking can be achieved by plasma etching. We believe the same fine-line patterns can be transferred into the Parylene using oxygen plasma etching.

We developed a scheme for patterning the Parylene as shown in figure 4. Parylene is chemical vapor deposited onto a substrate or existing structures (figure 4a). Next, the masking metal is evaporated or sputtered onto the Parylene surface (figure 4b). Photoresist is deposited and patterned (figure 4c) using conventional photolithographic techniques. The photoresist is used as an etch mask for chemical wet etching of the metal layer (figure 4d), and the Parylene is then etched in an oxygen plasma with the metal layer as a mask (figure 4e). During this step, the photoresist is also removed. Finally, the metal masking material is removed using the same wet etch process as previously, leaving the patterned Parylene structure (figure 4f).

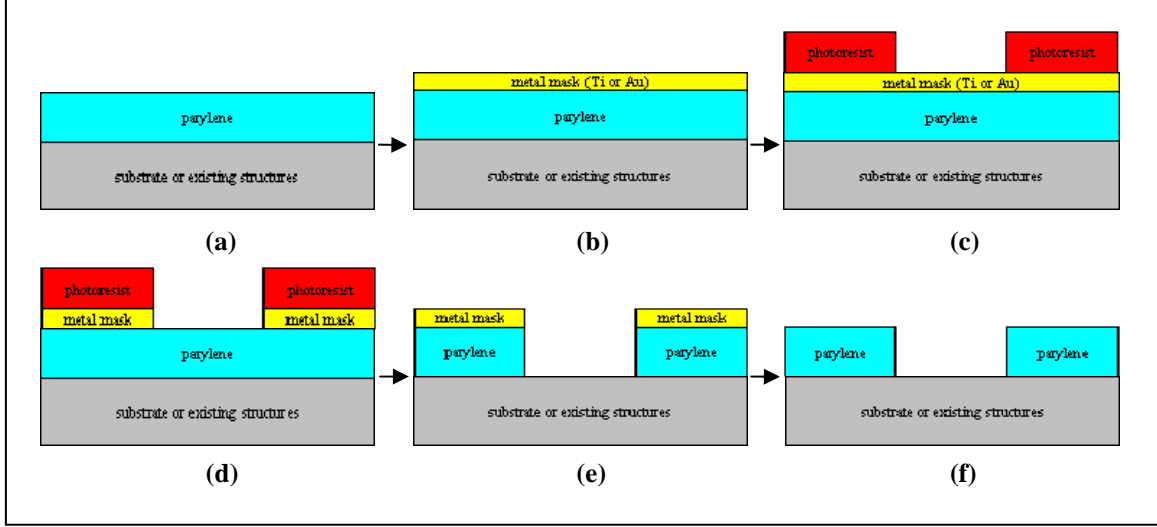


Figure 4. Process flow for patterning Parylene with a metal mask.

Plasma processes have been shown to work previously with aluminum (4, 5) and silicon oxide (6, 7). It is the goal of the present work to extend the research using plasma processes with gold (Au) and titanium (Ti) masks to evaluate the resolution of pattern transfer in different etch recipes and to integrate the process with an EFI structure.

2. Experiment/Calculations

Process development was divided into three distinct phases: (1) determination of an etch rate for Parylene in oxygen plasma, (2) determination of the feasibility of Au and Ti masking materials, and (3) characterization of the etch quality in different etch recipes. Different samples were prepared and evaluated for each of the phases.

2.1 Parylene Etch Rate Calculation

In the first phase, etch rate tests were conducted to determine if useful Parylene etch rates can be achieved using oxygen plasma and to facilitate etch time prediction for subsequent phases. The lithography patterning method was skipped during this phase, and instead a crude and fast approach was used to reduce the process steps and time needed to perform the analysis. No chemicals or alignments were used in this phase of the investigation other than the oxygen plasma itself. The Parylene films were prepared on 100-mm diameter polished silicon substrates. A polyimide tape was applied across the substrate followed by the Parylene deposition. A step height was created in the Parylene after carefully scoring the taped surface edge with a razor blade and lifting the tape until the underlying silicon substrate was exposed. About 15% of the total Parylene surface area was removed using the tape method. By putting down several tapes on one substrate, we were able to determine the amount of etched Parylene at

each etch time interval before all the material was completely removed. Some edge peeling was unavoidable with the razor blade method, so scan distances were sufficiently long as to avoid the edge effects.

The wafers were etched in multiple steps using two oxygen plasma recipes detailed in table 1. The intended plasma recipes were meant to produce both isotropic and anisotropic etch conditions. In the isotropic condition, the etched Parylene material eroded equally in all directions forming sloping sidewall cavities. In the anisotropic condition, the etching occurred faster in one direction and forming straight sidewalls. We used a commercial reactive ion etcher (RIE) for the anisotropic etching and a parallel plate oxygen plasma ashing system for the isotropic etching. Etch step times ranged from 5–10 min. After each etch step, the step height was re-measured at two points. In total, each wafer was etched in at least four steps, with step height measurements taken at two points after each step. To determine an etch rate, the two step heights were averaged to give an average step height, and linear least squares regression was conducted with cumulative etch time as the independent variable and average step height as the dependent variable. The etch rate was found as the negative of the slope of the linear least squares regression line.

Table 1. Oxygen plasma etch recipes tested.

Process Parameter	Isotropic Etch	Anisotropic Etch
Pressure	1000 mtorr	500 mtorr
O ₂ flow rate	500 sccm	50 sccm
Bias voltage	0 V dc	–540 V dc

2.2 Metal Masking Feasibility

In this second phase, tests were conducted to determine the survivability of Au or Ti metal masking materials to chemical processes and oxygen plasma. Mask patterning and alignment over the EFI structure was completed by the lithography method. The usefulness of the masking materials were evaluated on top of EFI structures consisting of Cu bridges with an overcoat of chromium (Cr) on a quartz substrate. These structures were coated with Parylene C by a contractor and later followed by either Ti (sputtered) or Au (e-beam evaporated) masking. Photoresist was spun onto the wafers, and exposed and developed in the positive mode using simple mask patterns (~2 mm diameter) dots. The Au metal mask was etched in an aqueous potassium iodide-iodine etching solution. Ti was etched in commercially available buffered oxide etch (BOE) solution. The Parylene on the test wafers was etched to completion using both isotropic and anisotropic oxygen plasma recipes as outlined in table 1. The voltage conditions were equivalent, but the oxygen pressure and flow varied intentionally to create the isotropic and anisotropic etch effects. The metal mask, after it is no longer needed, can be removed using the same aqueous etch chemicals as before. The processes were evaluated by optical and scanning electron microscopy (SEM).

2.3 Etch Characterization

In the third phase, characterization tests were designed to rigorously qualify the isotropic and anisotropic oxygen plasma etching, the extent of mask undercutting, and the achievability of a minimum feature size of the Parylene material. Based on the previous feasibility tests and poor reliability of the Ti mask, only the Au masking was investigated in this phase of the project. During this phase, Parylene was deposited on only plain polished 75-mm diameter silicon wafers. The Au film mask layer was intentionally selected to be thin and yet sufficient to cover up the roughness features of the underlying Parylene surface and not have open holes. The strategy here was also intended to reduce the etch time needed to remove the metal mask after completion of the Parylene etch. If the metal mask was made too thick, a longer etch time was needed that could possibly affect the other surrounding structure integrity. Photoresist was spun onto a wafer in the positive mode with patterns containing several features of interest ranging from 5–200 μm in size according to figure 5. The Au metal mask was etched in an aqueous potassium iodide-iodine etching solution. The Parylene was etched to completion. The wafers were then diced by hand into smaller pieces and examined with a SEM. The Au masking was intentionally kept intact to characterize the etched surfaces and determine the amount of etch undercutting.

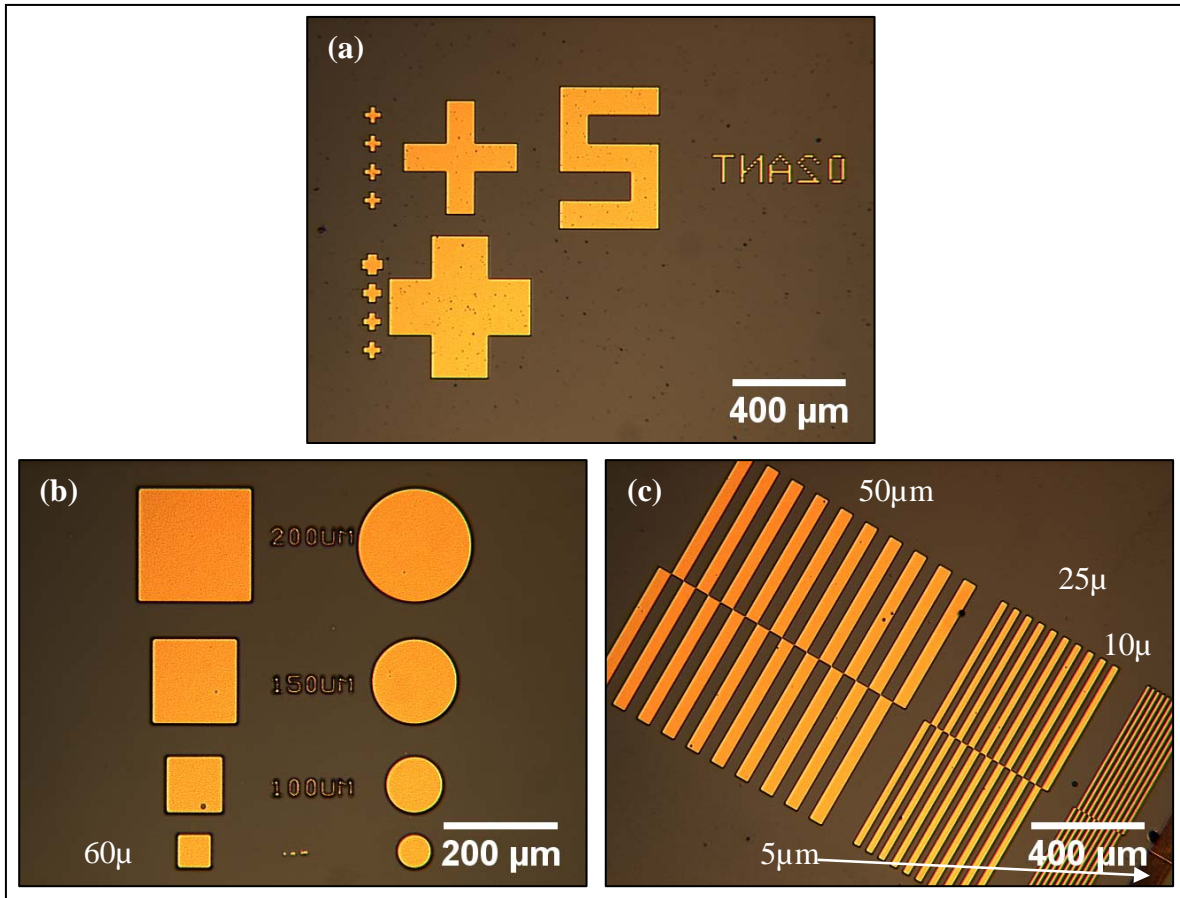


Figure 5. Optical microscope images of metal mask patterns on silicon substrate: (a) crosses, (b) squares and dots, and (c) lines.

3. Results and Discussion

3.1 Parylene Etch Rate Calculation

Plots of average step height versus time for the two etch recipes are shown in figure 6. A linear etch rate was predicted for Parylene etching in oxygen plasma. The data seemed to agree with this analysis, with linear regression producing values of $R^2 = 0.9859$ and $R^2 = 0.9982$ for the isotropic and anisotropic etch recipes, respectively. The etch rates were comparable, with a rate of 232 nm/min for the isotropic etch recipe and 245 nm/min for the anisotropic etch recipe. These values are similar to those obtained elsewhere (8, 9) using similar recipes. It was noted during etch rate testing that the Parylene tended to etch faster on the edges than in the center. This was most obvious near the end of the etch, as the edges of the Parylene surface would begin to recede shortly before etch completion. Consequently, the etch rates obtained were slightly on the low side. In practice, this error was easily corrected by adding about 5 min to the calculated etch time.

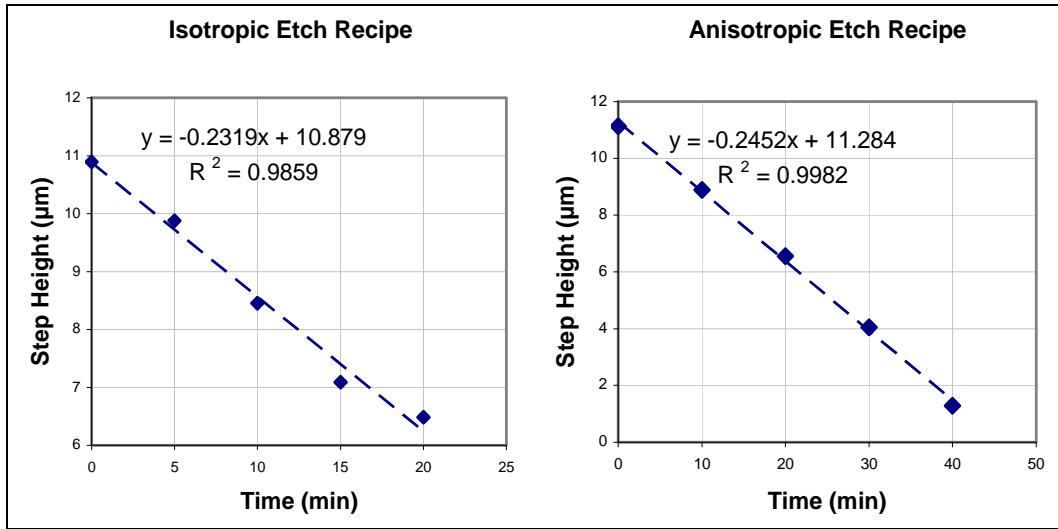


Figure 6. Plots of average Parylene step height versus time for (a) isotropic and (b) anisotropic etch recipe. Note the generally linear trend.

3.2 Metal Masking Material Feasibility

3.2.1 Ti Masking

Ti was rejected as a suitable masking material based on the initial feasibility tests conducted over sample EFI structures. A BOE solution was able to etch and pattern the Ti mask with no noticeable scarring or peeling of the Parylene, as shown in figure 7. However, during the second metal removal step (described in figure 4(e)), the BOE had a strong tendency to also peel up the unetched Parylene film along with the Ti. In the dot shaped mask test, some amount of peeling occurred along the edge of a Cu bridge, as in figure 8(a), and over 50% of the Parylene dots were

completely removed, as in figure 8(b). A second test, performed with an array of larger (~1 cm) Parylene square features, confirmed the problem. Although none of the square masks completely peeled off, they all exhibited some peeling on the edges of the Cu bridge structure. Such peeling undermines the effectiveness of the Parylene coating as a flyer material for EFI application.

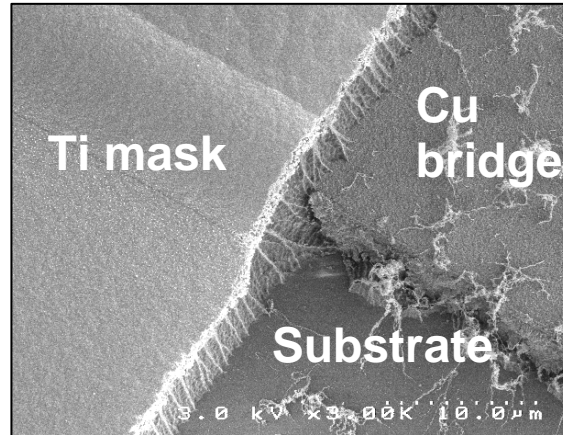


Figure 7. Scanning electron micrograph showing the edge of a Ti mask and underlying Parylene film after anisotropic oxygen plasma etch. Note good pattern transfer as well as good Parylene step coverage over the Cu bridge structure. Stringy clumps in the lower right are as yet unidentified etch residues, possibly related to etch chamber contamination.

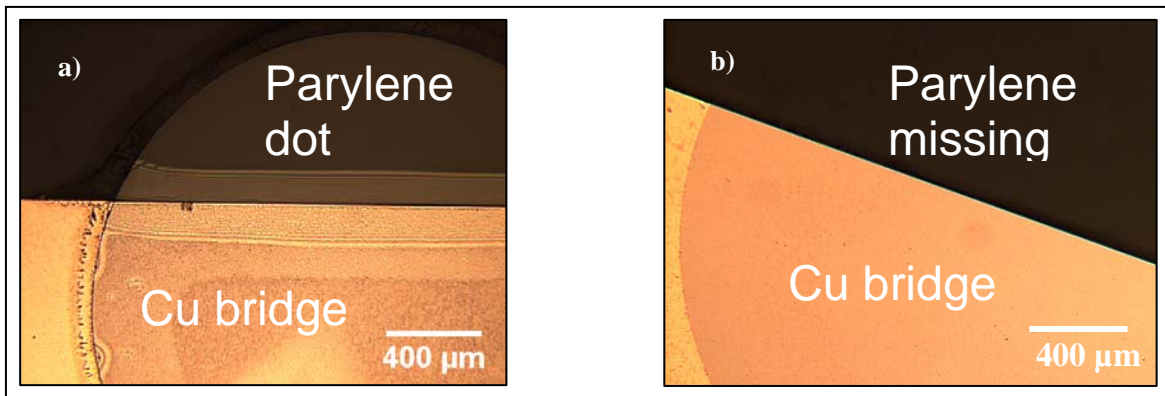


Figure 8. Optical microscope images showing complications after the process of removing the Ti mask. In (a), the dot patterned Parylene film shows striations and discoloration along the edge of a metal Cu bridge that are indicative of peeling, while in (b), the Parylene dot film has been completely removed.

3.2.2 Au Masking

Au etchant showed good compatibility with the mask. No peeling or scarring of the Parylene surface occurred when the Au was removed after the oxygen plasma etch. Based on these results, Au was chosen as the masking material for further investigation leading into the characterization phase.

Mask patterns with cross features were used to generalize the etch characteristics of both the isotropic and the anisotropic etch recipes. We paid attention to a particular set of mask dimensions noted in figure 9 for determining the minimum etch limits for the isotropic etch recipe.

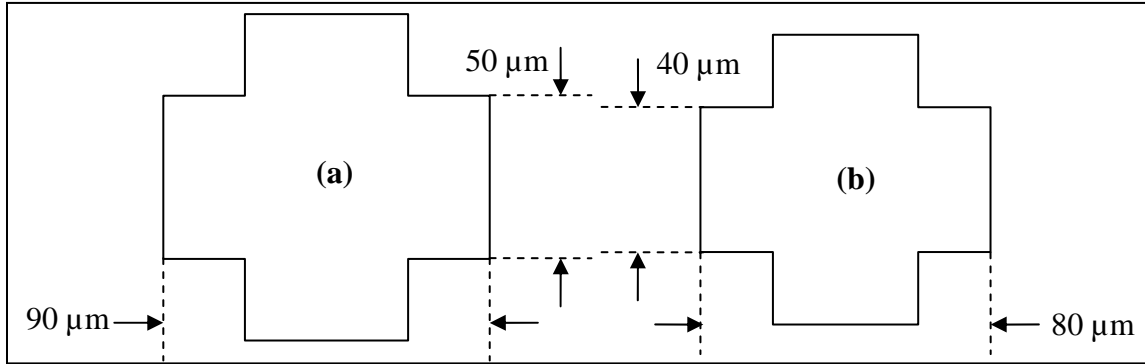


Figure 9. Dimensions of the mask cross patterns prior to etching. The upper cross (a) is slightly larger than the lower cross (b).

As can be seen from an overall mask perspective in figure 10(a) and the close-ups of the respective regions, all the patterns transferred successfully for the isotropic and anisotropic etch recipes. The isotropic etch recipe in figure 10(c) clearly produced more undercutting than the anisotropic recipe in figure 10(b). The Au mask introduced ripples around the edges where the undercutting occurred. The limitations of isotropic etching became more apparent with the smaller features. As a consequence, some smaller features failed to transfer due to total undercutting failure (figure 10e). Based on comparative observations between figure 9 and figure 10(e), we roughly estimated that the minimum feature achieved was $50\text{ }\mu\text{m}$ using the isotropic etch recipe for this thick film Parylene. The feature with the minimum size of $40\text{ }\mu\text{m}$ was not standing after completion of the isotropic etch.

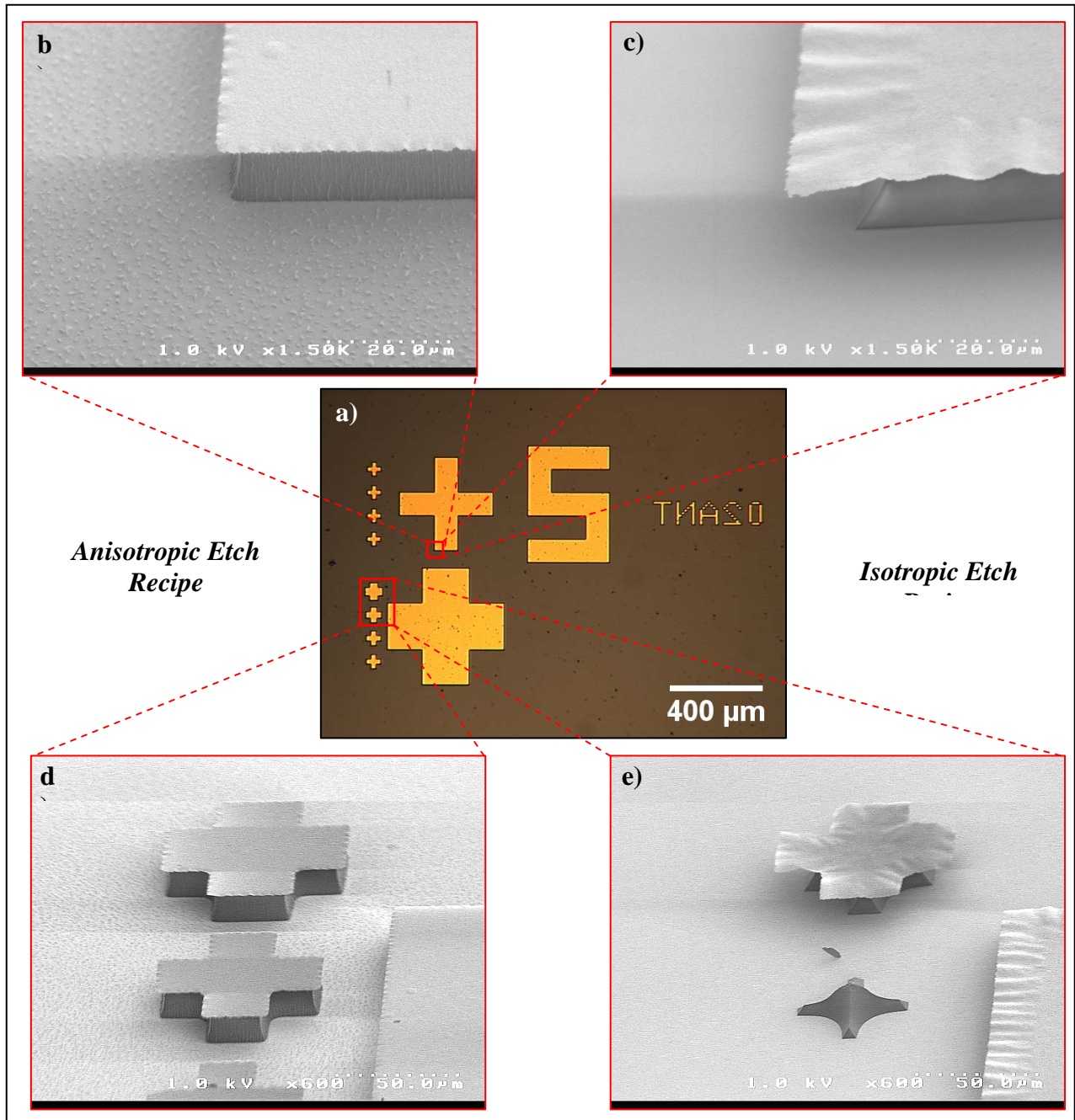


Figure 10. Micrographs illustrating varying degrees of etch undercutting below the Au mask: (a) optical microscope image showing the Au mask patterns prior to Parylene etching, (b) SEM corner of large cross pattern transfer after anisotropic etch, (c) the same corner after isotropic etch (note greater undercutting), (d) SEM of two smaller crosses after anisotropic etch, and (e) the same crosses after isotropic etch (the smaller cross has been completely undercut).

Another interesting observation we made regarding the isotropic etching was occasional cracking of the Parylene film. In the dot and square mask pattern, about 40 min into the isotropic etch, cracking of the Parylene layer was observed, as in figure 11. The cracks broke through the thin Au mask layer in many areas, and by the time most of the Parylene was removed, much of the

Au mask was flaking off and the sample was deemed unsuitable for SEM. While this phenomenon may require more investigation, initial assessment is that it was a result of a combination of heating effects and undercutting caused by over-etching. Parylene has been observed to crack under thermal stress (10), and significant undercutting was observed in the previous characterization test. Parylene etch rates in oxygen plasmas have been noted to be much less inside trenches and between dense features. This was confirmed here, as the edges etched relatively quickly, while the Parylene in the center of the wafer took much longer to etch. Most of the Au mask damage occurred during this extended period of over-etching needed to compensate for the differences, so the isotropic etch seems to be limited to patterning relatively large, low dense features.

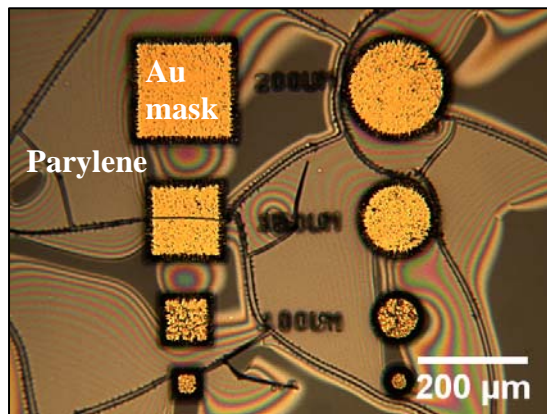


Figure 11. Cracking of Parylene film from the isotropic etch recipe. Multiple cracking is evident in the partially etched Parylene film as well as through the Au masking layer.

3.3 Etch Characterization

The initial assessment of the anisotropic etch recipe was that a wide variety of mask shapes can be transferred accurately on the order of 1 μm scale without damaging the Parylene, as shown in figure 12. A wide range of mask dimension for the square and dot patterns were still standing except for the ones approaching 1 μm. The final etched features were smaller in width compared to the mask dimensions. An example of this is shown in figure 13(a), where a set of 10-μm-wide line patterns appear to be standing but the width of the Parylene material is less than the mask standing above it. However, the next smaller set of 5-μm-wide line patterns in figure 13(b) appear collapsed. The effects of undercutting became pronounced with decreasing mask dimensions. The minimum achievable etch feature size for the anisotropic etch recipe was estimated to be approximately 10 μm, near the same order of magnitude as the thick film Parylene.

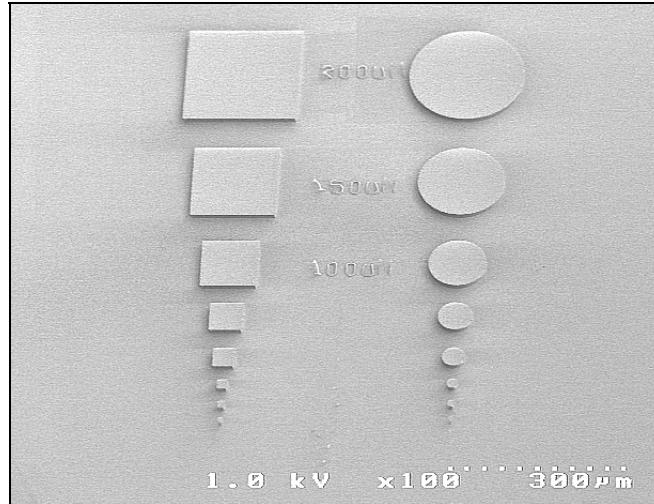


Figure 12. Scanning electron micrograph overview of anisotropically etched features 200, 150, 100, 60, 40, 20, 10, and 5 μm (from top to bottom).

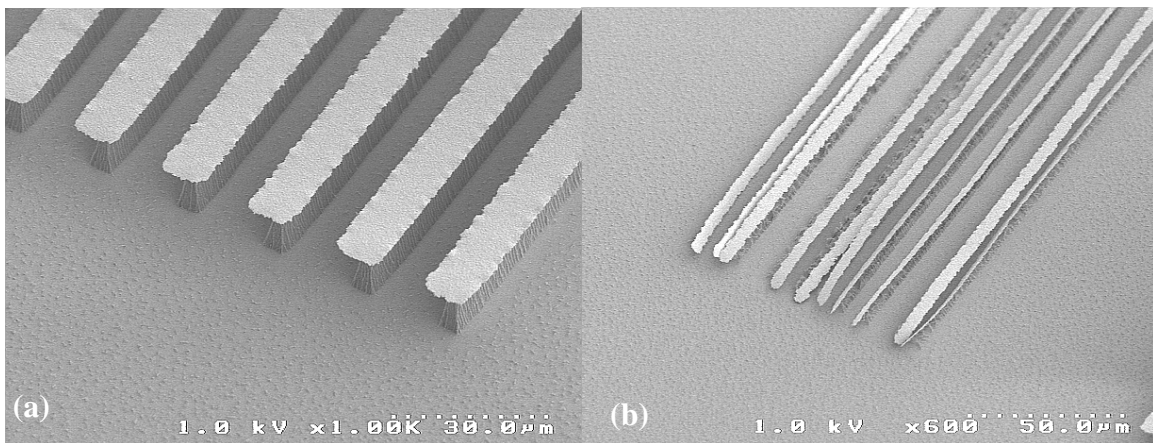


Figure 13. Scanning electron micrographs depicting the approximate minimum feature size of line patterns after anisotropic etch: (a) 1000 times magnification of 10- μm -wide lines and (b) 600 times magnification of 5- μm -wide lines.

3.4 Outstanding Issues

While oxygen plasma is generally thought to etch polymers primarily, during the feasibility tests it noticeably attacked a Cr protective top layer of the EFI structure in both etch recipes, in some cases exposing the bulk Cu layer. This is a concern for compatibility with the existing process, but was still under investigation at the time of this report. Metal etching in oxygen plasmas has been documented elsewhere (11), but not with Cr and not at the rates that would be required to remove the Cr layer. It is possible that the outdated nature of the wafers received from a contracted facility during the feasibility tests introduced unknown variables into the process.

Another as yet unexplained issue is the presence of small, stringy clumps of material on the etched surface of all samples in figure 7 etched using the anisotropic etch recipe. The occurrence of surface roughness and “grass” has been documented previously after oxygen plasma RIE of Parylene (12), but these observations were made on incompletely etched Parylene, and the resolution of the SEM images provided in that publication does not permit detailed comparison. It was postulated by Majid that the surface roughness was due to preferential etching in areas where the polymer is weak, but if that were the case one would not expect to see this phenomenon when doing complete Parylene removal. Additional oxygen plasma treatment of surfaces covered with the clumps had no noticeable effect. Cleaning with organic solvents and BOE was also attempted, again with no effect. It was also speculated that the clumps were due to etch chamber contamination.

4. Summary and Conclusions

A method for patterning thick film Parylene has been investigated. The etch rates and degree of anisotropy have been assessed for two different oxygen plasma etch recipes, and approximate minimum feature sizes have been obtained for each recipe. Preliminary compatibility studies have been conducted to determine the compatibility of an Au masking layer with EFI structures. Remaining obstacles to the integration of oxygen plasma Parylene removal into the existing process flow for the EFI structure have been identified, and potential next steps have been suggested. Based on these results Au masking and oxygen plasma shows great promise as an option for selective Parylene patterning for flyer material application.

5. References

1. Specialty Coating Systems. *Discovery and Early History of Parylene*. http://www.scscoatings.com/parylene_knowledge/history.aspx. (accessed 21 July 2008).
2. Gazicki-Lipman, M. Vapor Deposition Polymerization of para-Xylylene Derivatives—Mechanism and Applications. *Journal of the Vacuum Society of Japan* **June 2007**, 50, 601–608.
3. Schmidt, E. M.; Bak, M. J.; Christensen, P. Laser Exposure of Parylene-C Insulated Microelectrodes. *Journal of Neuroscience Methods* **April 1995**, 62, 89–92.
4. Mastrangelo, C. H.; Saloka, G. S. A Dry-Release Method Based on Polymer Columns for Microstructure Fabrication. *Proc. of 1993 IEEE Conf. on MEMS*, 77–81, February 1993.
5. Zahn, J. D.; Gabriel, K. J.; Fedder, G. K. A Direct Plasma Etch Approach to High Aspect Ratio Polymer Micromachining with Applications in BioMEMS and CMOS-MEMS. *Proc. of 15th Intn'l IEEE Conf. on MEMS*, 137–140, January 2002.
6. Tacito, R. D.; Steinbrüchel, C. Fine-Line Patterning of Parylene-n by Reactive Ion Etching for Application as an Interlayer Dielectric. *Journal of the Electrochemical Society* **June 1996**, 143, 1974–1977.
7. Yeh, J.T.C.; Grebe, K. R. Patterning of Poly-pary-xylylenes by Reactive Ion Etching. *Journal of Vacuum Science and Technology A* **June 1983**, 1, 604–608.
8. Meng, E.; Tai, Y. Parylene Etching Techniques for Microfluidics and BioMEMS. *Proc. of 18th Intn'l. IEEE Conf. on MEMS*, 568–571, February 2005.
9. Williams, K. R.; Gupta, K.; Wasilik, M. Etch Rates for Micromachining Processing—Part II. *Journal of Microelectromechanical Systems* **December 2003**, 12, 761–778.
10. Hsu, J.; Kammer, S.; Jung, E.; Rieth, L.; Normann, A. R.; Solzbacher, F. Characterization of Parylene-C Film as an Encapsulation Material for Neural Interface Devices. *Proc. of the 3rd Intn'l Conf. on Multi-Material Micro Manufacture*, 2007.
11. Chou, C. H.; Philips, J. Platinum Metal Etching in a Microwave Oxygen Plasma. *Journal of Applied Physics* **September 1990**, 68, 2415–2423.
12. Majid, N.; Dabral, S.; McDonald, J. F. The Parylene-Aluminum Multilayer Interconnection System of Wafer Scale Integration and Wafer Scale Hybrid Packaging. *Journal of Electronic Materials* **March 1989**, 18, 301–311.

List of Symbols, Abbreviations, and Acronyms

Au	gold
Cr	chromium
Cu	copper
EFI	exploding foil initiator
BOE	buffered oxide etch
MEMS	microelectromechanical systems
RIE	reactive ion etcher
SEM	scanning electron microscopy
Ti	titanium

NO. OF COPIES	ORGANIZATION	NO. OF COPIES	ORGANIZATION
1 ELEC	ADMNSTR DEFNS TECHL INFO CTR ATTN DTIC OCP 8725 JOHN J KINGMAN RD STE 0944 FT BELVOIR VA 22060-6218	1	US ARMY RSRCH LAB ATTN RDRL CIM G T LANDFRIED BLDG 4600 ABERDEEN PROVING GROUND MD 21005-5066
1	DARPA ATTN IXO S WELBY 3701 N FAIRFAX DR ARLINGTON VA 22203-1714	12	US ARMY RSRCH LAB ATTN IMNE ALC HRR MAIL & RECORDS MGMT ATTN RDRL CIM L TECHL LIB ATTN RDRL CIM P TECHL PUB ATTN RDRL SER E P AMIRTHARAJ ATTN RDRL SER L B PIEKARSKI ATTN RDRL SER L B ROD ATTN RDRL SER L E ZAKAR ATTN RDRL SER L L CURRANO ATTN RDRL SER L M DUBEY ATTN RDRL SER L R POLCAWICH ATTN RDRL SER L W CHURAMAN ATTN RDRL SES S B MARY ADELPHI MD 20783-1197
1 CD	OFC OF THE SECY OF DEFNS ATTN ODDRE (R&AT) THE PENTAGON WASHINGTON DC 20301-3080	5	US ARMY TACOM-ARDEC ATTN RDAR MEF FA D ERRERA ATTN RDAR MEF FA J D CAMPBELL ATTN RDAR MEF FA C ROBINSON ATTN RDAR MEF FA J F HARTRANFT ATTN RDAR MEF FA W KONICK ADELPHI MD 20783-1197
1	US ARMY RSRCH DEV AND ENGRG CMND ARMAMENT RSRCH DEV AND ENGRG CTR ARMAMENT ENGRG AND TECHNLGY CTR ATTN AMSRD AAR AEF T J MATTS BLDG 305 ABERDEEN PROVING GROUND MD 21005-5001		
1	PM TIMS, PROFILER (MMS-P) AN/TMQ-52 ATTN B GRIFFIES BUILDING 563 FT MONMOUTH NJ 07703		
1	US ARMY INFO SYS ENGRG CMND ATTN AMSEL IE TD A RIVERA FT HUACHUCA AZ 85613-5300		
1	COMMANDER US ARMY RDECOM ATTN AMSRD AMR W C MCCORKLE 5400 FOWLER RD REDSTONE ARSENAL AL 35898-5000		
1	US GOVERNMENT PRINT OFF DEPOSITORY RECEIVING SECTION ATTN MAIL STOP IDAD J TATE 732 NORTH CAPITOL ST NW WASHINGTON DC 20402		
			TOTAL: 26 (1 ELEC, 1 CDS, 24 HCS)